mAbs 6:4, 1026–1037; July/August 2014; © 2014 Landes Bioscience

Highly potent anti-CD20-RLI immunocytokine targeting established human B lymphoma in SCID mouse

Marie Vincent[1], Géraldine Teppaz[1], Laurie Lajoie[2], Véronique Solé[1], Anne Bessard[1], Mike Maillasson[1], Séverine Loisel[3], David Béchard[4], Béatrice Clémenceau[5,6], Gilles Thibault[2], Laure Garrigue-Antar[1], Yannick Jacques[1,†], and Agnès Quéméner[1,†]

[1]UMR892-INSERM, 6299-CNRS; Université de Nantes; équipe Cytokines et Récepteurs en Immuno-Cancérologie; Nantes, France; [2]UMR7292-CNRS; Université François Rabelais de Tours and Centre Hospitalier Universitaire de Tours; Laboratoire d'Immunologie; Tours, France; [3]EA2216 and IFR148; University Medical School; Université Européenne de Bretagne; Brest, France; [4]Cytune Pharma SAS; Nantes, France; [5]UMR892-INSERM, 6299-CNRS; Université de Nantes, équipe Immunothérapie; Nantes, France; [6]Centre Hospitalier Universitaire de Nantes; Nantes, France

[†]These authors contributed equally to this work.

Keywords: interleukin-15, CD20, Rituximab, immunocytokine, cancer therapy, lymphoma, B cell malignancies

Abbreviations: RTX, rituximab; ICK, immunocytokine; ADCC, antibody-dependent cellular cytotoxicity; CDC, complement-dependent cytotoxicity; NHL, follicular non-Hodgkin's lymphoma; CLL, chronic lymphocytic leukemia; SCID, severe combined immunodeficiency; IL, interleukin; mAb, monoclonal antibody; p-STAT5, phospho-STAT5; R, reducing; NR, non-reducing; SPR, surface plasmon resonance

Rituximab (RTX), a chimeric IgG1 monoclonal antibody directed against the CD20 antigen, has revolutionized the treatment of B-cell malignancies. Nevertheless, the relapsed/refractory rates are still high. One strategy to increase the clinical effectiveness of RTX is based on antibody-cytokine fusion protein (immunocytokine; ICK) vectorizing together at the tumor site the antibody effector activities and the cytokine co-signal required for the generation of cytotoxic cellular immunity. Such ICKs linking various antibody formats to interleukin (IL)-2 are currently being investigated in clinical trials and have shown promising results in cancer therapies. IL-15, a structurally-related cytokine, is now considered as having a better potential than IL-2 in antitumor immunotherapeutic strategies. We have previously engineered the fusion protein RLI, linking a soluble form of human IL-15Rα-sushi+ domain to human IL-15. Compared with IL-15, RLI displayed better biological activities in vitro and higher antitumor effects in vivo in murine and human cancer models. In this study, we investigated the advantages of fusing RLI to RTX. Anti-CD20-RLI kept its binding capacity to CD20, CD16 and IL-15 receptor and therefore fully retained both antibody effector functions (ADCC and CDC), and the cytokine potential of RLI. In a severe combined immunodeficiency (SCID) mouse model of disseminated residual lymphoma, anti-CD20-RLI was found to induce long-term survival of 90% of mice up to at least 120 days whereas RLI and RTX, alone or in combination, just delayed the disease onset (100% of death at 28, 40 and 51 days respectively). These findings suggest that such ICK could improve the clinical efficacy of RTX, particularly in patients with refractory B-cell lymphoma.

Introduction

Rituximab (RTX), a chimeric monoclonal antibody (mAb) directed against the CD20 antigen, is currently used associated with chemotherapy for the treatment of follicular non-Hodgkin's lymphoma (NHL), diffuse large B cell lymphoma[1] and chronic lymphocytic leukemia (CLL).[2] CD20 is a non-glycosylated trans-membrane protein of 33 to 37kDa that is expressed on the surface of normal B cells from pre-B to mature-B cell stage, but not on hematopoietic stem cells, progenitor B cells or plasmocytes.[3] In B cell malignancies, like B cell NHL, CD20 is highly expressed. Because CD20 is not down-modulated and rarely shed,[4] it represents a good target for antibody-based immunotherapy. RTX binding to CD20 can lead to cell lysis through several mechanisms including apoptosis, antibody dependent cell-mediated cytotoxicity (ADCC), phagocytosis and complement-mediated cytotoxicity (CDC).[5] Relapse or absence of clinical response after RTX treatment is however significant, and ~half of the patients who receive it do not respond to RTX treatment, probably because of the development by B cells of RTX resistance, including a decrease of ADCC or CDC.[6,7] Thus, several studies have aimed at enhancing the functional activities of anti-CD20 antibodies by increasing their binding to CD16a

*Correspondence to: Agnès Quéméner; Email: agnes.quemener@inserm.fr; Yannick Jacques; Email: Yannick.Jacques@univ-nantes.fr
Submitted: 02/07/2014; Revised: 03/28/2014; Accepted: 03/28/2014; Published Online: 04/07/2014
http://dx.doi.org/10.4161/mabs.28699

(FcγRIIIa),[8,9] a receptor responsible for ADCC and expressed on NK cells, neutrophils and macrophages.[10]

An alternative approach to increase the effects of RTX is based on its combination with agents that stimulate ADCC-competent immune effector cells. Interleukin (IL)-2 is one of these agents; it is a potent stimulator of both T and NK cells, and has already been tested in association with RTX in pre- and Phase 1 clinical studies.[11,12] In such a context, an antibody-cytokine fusion protein (immunocytokine; ICK) linking an anti-CD20 antibody to IL-2 has been developed and was shown to display higher antitumor activity compared with the corresponding naked antibody, in a severe combined immmunodeficient (SCID) mouse model of disseminated residual human lymphoma.[13]

Among the most advanced ICKs targeting tumor antigens and using various pro-inflammatory cytokines, those based on IL-2 have shown promising results in Phase 2 clinical trials, but with adverse effects resembling the ones observed with recombinant IL-2.[14,15] Although displaying similar in vitro effects, IL-15, a cytokine structurally related to IL-2, is considered as having a better potential in antitumor immunotherapeutic strategies, and has been shown to be 6 times less toxic than IL-2 in preclinical studies.[16] To mediate its actions, IL-15 binds to a receptor that shares with the IL-2 receptor the IL-2/IL-15Rβ and common γ chains as transducing components. In addition, IL-2 and IL-15 each uses a private α chain (IL-2Rα and IL-15Rα) that confers cytokine specificity and enhances the affinity of cytokine binding.[17,18] The mechanism of action of IL-15 in vivo, playing a major role in tumor immunosurveillance, relies on its *trans*-presentation by IL-15 producer cells expressing IL-15Rα (dendritic cells, macrophages and epithelial cells) to responder cells (NK or memory $CD8^+$ T cells) bearing the IL-15Rβ/γ receptor.[19-21] IL-15 is particularly crucial for the development of innate immune cells, the cellular activation of T and NK cells, and the survival of $CD8^+$ memory T cells.[22,23] Unlike IL-2, IL-15 does not induce activation-induced cell death (AICD) of $CD8^+$ effectors cells[24] and does not seem to exert an important influence on regulatory T cells that can dampen the antitumor immune responses.[25] Furthermore, IL-15 has been shown to increase the ADCC activity of RTX against a lymphoma B cell line and against lymphoma cells from CLL patients.[26,27] Recently, IL-15 *trans*-presentation by B leukemic cells from CLL patients has been demonstrated in vitro and was shown to stimulate and expand autologous NK cells and to lead to B leukemic cell depletion, a process greatly amplified in the presence of mAbs such as RTX or GA101 (an optimized anti-CD20 antibody).[28]

We previously described the existence of a soluble form of the human IL-15Rα that results from the proteolytic cleavage of membrane-anchored IL-15Rα by metalloproteases.[29] Several studies have subsequently revealed the higher stimulatory effects of soluble IL-15Rα/IL-15 complexes over IL-15 alone in vitro and in vivo.[30-32] Accordingly, we previously engineered a fusion protein (RLI), that consists of the NH2-terminal (amino acids 1–77, sushi+) domain of IL-15Rα linked via a 20-amino acid linker to IL-15.[33] RLI was shown to exert higher biological activities than IL-15 or even the non-covalent association of IL-15 with the soluble IL-15Rα to drive in vitro cell proliferation through the IL-15Rβ/γ receptor,[34] and to promote in vivo mobilization and expansion of NK cells.[35] Moreover, when injected in mice, RLI displayed an increased serum half-life compared with IL-15 and revealed strong antitumor effects depending mainly on the NK cell subset, in systemic B16 melanoma mouse model and human HCT-116 colorectal cancer.[36]

We therefore aimed at engineering RLI-based ICKs that could combine the tumor targeting and cytotoxic properties of therapeutic mAbs, and the immune stimulating potencies of RLI (**Fig. 1**). Such an ICK was first built on the basis of an antibody targeting GD2, a sialic acid-bearing glycosphingolipids expressed on many human neurectodermal tumors. Anti-GD2-RLI was shown to extend mice survival in a lymphoma mouse model and to decrease metastatic progression in a syngenic immunocompetent murine model of cancer.[37] Here, we describe the biological activities in vitro and the high anti-tumor potencies in vivo of a RLI-based ICK targeting the CD20 antigen, highlighting the potential therapeutic benefit of such fusion proteins in B cell malignancies.

Results

Characterization of the anti-CD20-RLI ICK

ICK construction is depicted in **Figure 2A**. The anti-CD20-RLI ICK was produced in transiently transfected CHO cells and purified by Protein A affinity chromatography. SDS-PAGE analysis under non-reducing (NR) conditions revealed major bands of 150 and 200kDa for RTX and anti-CD20-RLI respectively, corresponding to the predicted molecular masses of the antibody and the fusion protein, with similar high degrees of purity (**Fig. 2B**, left panel). SDS-PAGE under reducing (R) conditions revealed two bands of 75 and 25kDa corresponding respectively to the heavy chain of RTX fused with RLI and the light chain of RTX (**Fig. 2B**, middle panel). The identity of anti-CD20-RLI heavy and light chains was further established by western blot analysis with an anti-IgG mAb (**Fig. 2B**, right panel, line 1) and the anti-IL-15 B-E29 mAb (**Fig. 2B**, right panel, line 2, heavy chain). The gel-filtration profile under native conditions showed that the recombinant fusion protein is mainly a monomer with some little propensity of dimer and trimer formation (**Fig. 2C**).

Binding of anti-CD20-RLI to CD20 and IL-15R was analyzed by flow cytometry. It bound to $CD20^+$ Raji cells with a similar mean binding level as RTX (**Fig. 3A**, left panel). Raji cells did not bind the irrelevant anti-GD2-RLI ICK, excluding that part of the anti-CD20-RLI reactivity was through its cytokine moiety. Anti-CD20-RLI was also able to bind to Kit225 cells that express endogenous IL-15Rα, IL-15Rβ and IL-15Rγ chains (**Fig. 3A**, middle panel) and to 32Dβ cells that express endogenous IL-15Rβ and IL-15Rγ chains (**Fig. 3A**, right panel). By contrast, no binding was detected for RTX, indicating in that case that anti-CD20-RLI bound through its cytokine moiety.

Binding of anti-CD20-RLI ICK to FcγRIIIa (CD16a) expressed on the surface of NK-92-$CD16^+$ cells[38] was also studied and compared with that of RTX. It was evaluated by measuring the inhibition of the binding of the FITC-conjugated anti-CD16a

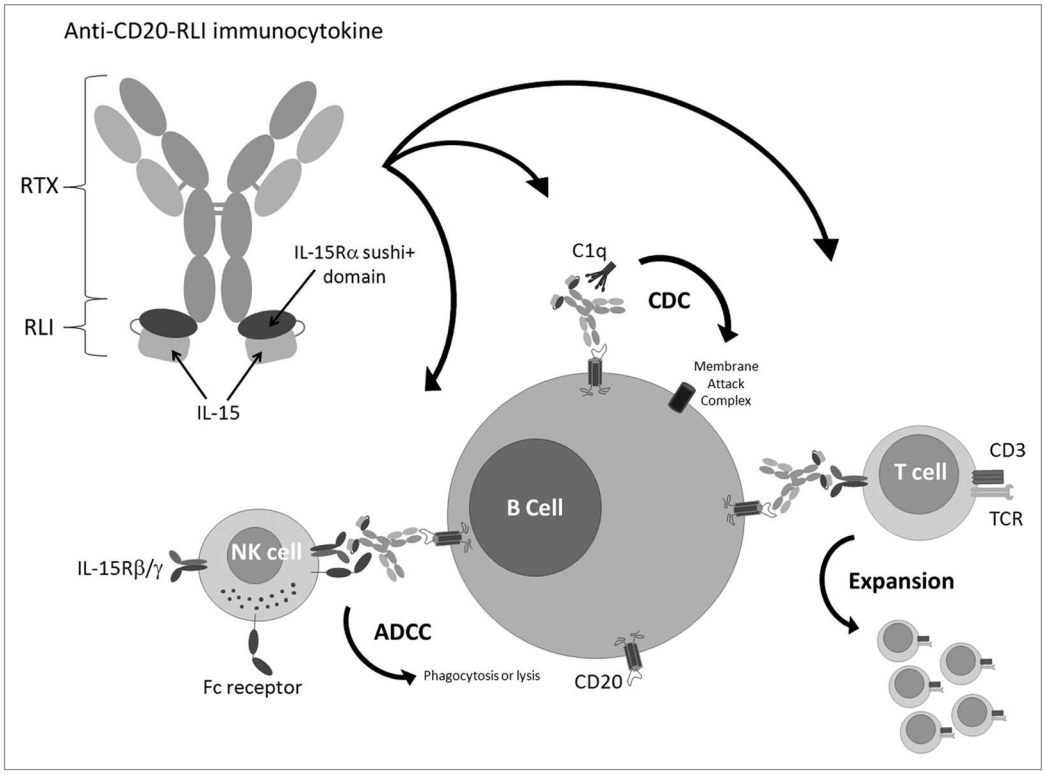

Figure 1. A RLI-based immunocytokine targeting the CD20 antigen and its potential mechanisms of action. RLI was fused to the C-terminus of the anti-CD20 antibody (RTX) heavy chain. The use of such fusion protein presents the advantages to trigger at the tumor site (B cell malignancies) the cytotoxic effector functions of the anti-CD20 antibody moiety together with the cytokine co-signal required for the generation of cytotoxic cellular immunity while avoiding the toxicities associated with systemic cytokine delivery.

mAb 3G8 to NK-92-CD16$^+$ cells. Similar inhibition curves were obtained with anti-CD20-RLI, RTX alone or in association with RLI (**Fig. 3B**), 80% inhibitory effects being achieved with 10 μM of mAbs. By contrast, RLI did not affect the binding of 3G8 mAb to CD16a (**Fig. 3B**).

Kinetic analysis by surface plasmon resonance (SPR) of the binding of anti-CD20-RLI to soluble immobilized IL-15Rβ/γ complex (**Fig. 3C**) was also performed and compared with that of RLI. As expected, RLI bound to IL-15Rβ/γ with an affinity in the nanomolar range (k on = 3.5×10^5 M^{-1} s^{-1}; k off = 7.6×10^{-4} s^{-1}; K_d = 2.2nM). The anti-CD20-RLI also bound to IL-15Rβ/γ, but with an about 3-fold-higher affinity mainly due to a decrease in the off rate (k on = 2.4×10^5 M^{-1} s^{-1}; k off = 1.7×10^{-4} s^{-1}; K_d = 0.72nM).

Cytokine activities

In agreement with previous reports,[33,34,39] IL-15 and RLI induced the proliferation of Kit225 cells through IL-15Rα/β/γ at similar low concentrations ($ED_{50} \approx$ 80 and 35pM, respectively) (**Fig. 4A**). On these cells, anti-CD20-RLI showed a dose-response effect similar to that of RLI ($ED_{50} \approx$ 36pM). On 32Dβ cells that express IL-15Rβ/γ, and as expected from our previous reports,[37] RLI was about 10-fold more efficient than IL-15 in inducing proliferation (ED_{50} = 122 vs 1259pM respectively, **Fig. 4B**). In this case, the anti-CD20-RLI ICK was found to exhibit an even higher (7-fold) potency (ED_{50} = 18pM) than RLI. A similar increased potency over RLI was already found in the case of anti-GD2-RLI, another RLI-based ICK.[37] Any potential participation of the anti-CD20 moiety of the ICK in its higher activity was ruled out by the fact that: (1) 32Dβ cells did not express CD20 under flow cytometric analysis; (2) RTX alone did not induce their proliferation; (3) the effect of the ICK was not modified by a saturating concentration of RTX (100 nM) (not shown).

Detection of STAT5 phosphorylation in 32Dβ cells

Phosphorylation of STAT5 was evaluated in 32Dβ cells, stimulated either with IL-15, RLI or anti-CD20-RLI. Consistent with our proliferation results, RLI was about 12-fold more efficient than IL-15 in inducing the phosphorylation of STAT5 (ED_{50} = 196 vs 2475pM, respectively, **Figure 4C**), and the anti-CD20-RLI ICK was found to be 7-fold more potent than RLI (ED_{50} = 28pM, **Fig. 4C**).

Antibody effectors functions

CDC was evaluated on the CD20$^+$ Daudi target cells. Cells were incubated either with RTX, anti-CD20-RLI or anti-GD2 as negative control, in the presence of human serum as a source of complement. Anti-CD20-RLI induced similar CDC as RTX (**Fig. 5A**). Its effect was even slightly better on a molar basis than that induced by the parental mAb. The specificity was assessed by the absence of cytotoxicity when using the irrelevant antibody anti-GD2 (**Fig. 5A**) and when using heat-inactivated serum (not shown). ADCC was evaluated on the CD20$^+$ Raji target cells, using purified NK cells from healthy donors as effector cells. Raji

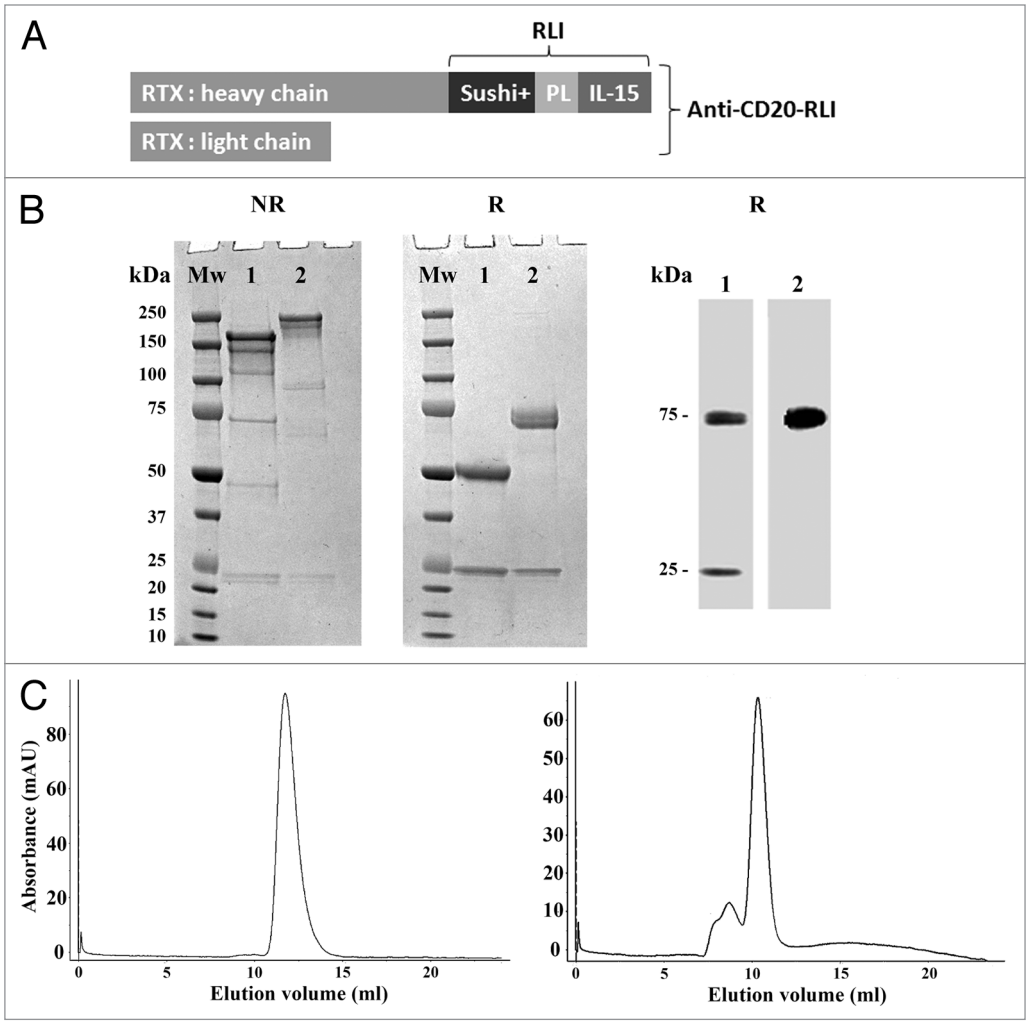

Figure 2. Production and purification of the anti-CD20-RLI ICK. **(A)** ICK construction, PL: Peptidic Linker within RLI fusion protein.[33] **(B)** SDS-PAGE under non reducing (left panel) and reducing (middle panel) conditions (Lane 1: 5 μg of RTX, line 2: 5 μg of anti-CD20-RLI); western blot analysis using anti-IgG Ab (right panel, line 1: 0.1 μg of anti-CD20-RLI) or anti-IL-15 Ab (right panel, line 2: 0.1 μg of anti-CD20-RLI). kDa: kilo Dalton; Mw: Molecular weight. **(C)** gel-filtration analysis of RTX (left panel) or affinity-purified anti-CD20-RLI (right panel) revealing mainly monomer.

cells were incubated either with RTX, RTX + RLI, anti-CD20-RLI, anti-GD2 or RLI, the latter two being used as negative controls. The effects were both effector-to-target cell (E/T) ratio-dependent (not shown) and dose-dependent (**Fig. 5B**). Anti-CD20-RLI induced a similar maximal ADCC as RTX alone or associated with RLI, although it was somewhat less efficient than RTX on a molar basis (EC_{50} = 26 pM vs 11 pM, respectively). No cytotoxic activity was observed with RLI, and the anti-GD2 antibody showed only background lysis, thereby demonstrating the antigen specificity of the assay.

ADCC was further investigated on $CD19^+$ B cell depletion from whole blood of healthy donors. Similar dose-dependent depletion curves and maximal effects were obtained with anti-CD20-RLI and RTX (**Fig. 6**). $CD3^+$ T cells and $CD56^+$ NK cells remained unaffected, demonstrating the $CD19^+$ B cell specificity of the assay (not shown). RLI did not induce $CD19^+$ cells depletion, nor did it interfere with the depleting effect of RTX (**Fig. 6**).

The activities of ICK and RTX were further compared on NK-cell activation by measuring in vitro CD16a down-modulation and NK-cell degranulation (CD107-based assay), using PMA/CaI treatment as positive control. Anti-CD20-RLI induced 2- to 3-fold higher CD16 down-modulation (**Fig. 7A**) and CD107 expression (**Fig. 7B**) on isolated human NK cells than RTX, at all incubation periods studied. RLI used alone had minor or no detectable effect.

Pharmacokinetics

Male C57BL/6 mice were injected intraperitonaly (i.p.) with a single equimolar (80 pmol) dose of anti-CD20-RLI (16 μg), or RTX (12 μg) (**Fig. 8** and **Table 1**). Plasma levels were determined using two ELISAs specific for human IgG or human IgG-IL-15 complex, respectively. For the ICK, both ELISAs gave similar results throughout the experiments, indicating that there was no significant alteration of the integrity of the anti-CD20-RLI fusion protein for at least 300 h after i.p. administration. The pharmacokinetic profile of RTX (half-life = 100h) was in agreement with previous

reports in mouse (half-life around 70 h)[40] and human (half-lives of 76 to 206 h).[41] In comparison, anti-CD20-RLI showed a strongly reduced bioavailability. Although displaying a similar maximal peak of plasma concentration (Cmax about 50 nM) as the parental antibody, its half-life (8.5 h) and AUC (1188 nM.h) were found 6- to 12-fold lower than those of RTX (100 h and 7770 nM.h, respectively). Nevertheless, the pharmacokinetic parameters of anti-CD20-RLI were far higher than those previously measured for RLI alone (3 h and 35 nM.h),[36] indicating that the fusion procedure markedly enhanced the bioavailability of RLI (**Table 1**).

Anti-tumoral activity of anti-CD20-RLI

The antitumoral efficacy of RTX and anti-CD20-RLI were compared in a Raji xenograft model. Raji proliferation in vitro was not affected by either IL-15 or RLI, therefore ruling out any potential direct effect of the RLI moiety on the tumor cells (data not shown). The mice survival curves were plotted according to Kaplan-Meier method and compared using log-rank test (**Fig. 9**). RLI alone at 2 μg did not significantly modify the median survival (23 d compared with 21 d for vehicle treated mice, **Fig. 9B**). RTX at an equimolar amount (12 μg) was slightly effective, by increasing the median survival rate to 27 d (**Fig. 9B**). Injection of a higher dose (200 μg, equivalent to 375 mg/m^2, a dose routinely used in human)[42] did not induce a greater effect (**Fig. 9A**). However, the association of RLI to RTX enhanced its protective effect (median survival of 37 d). Unexpectedly, the antigen-irrelevant anti-GD2-RLI ICK also resulted in an increase of the median survival (52 d). However, and spectacularly, treatment with the equimolar amount of anti-CD20-RLI (16 μg) resulted in long-term survival of 90% of mice up to at least 120 d (**Fig. 9B**).

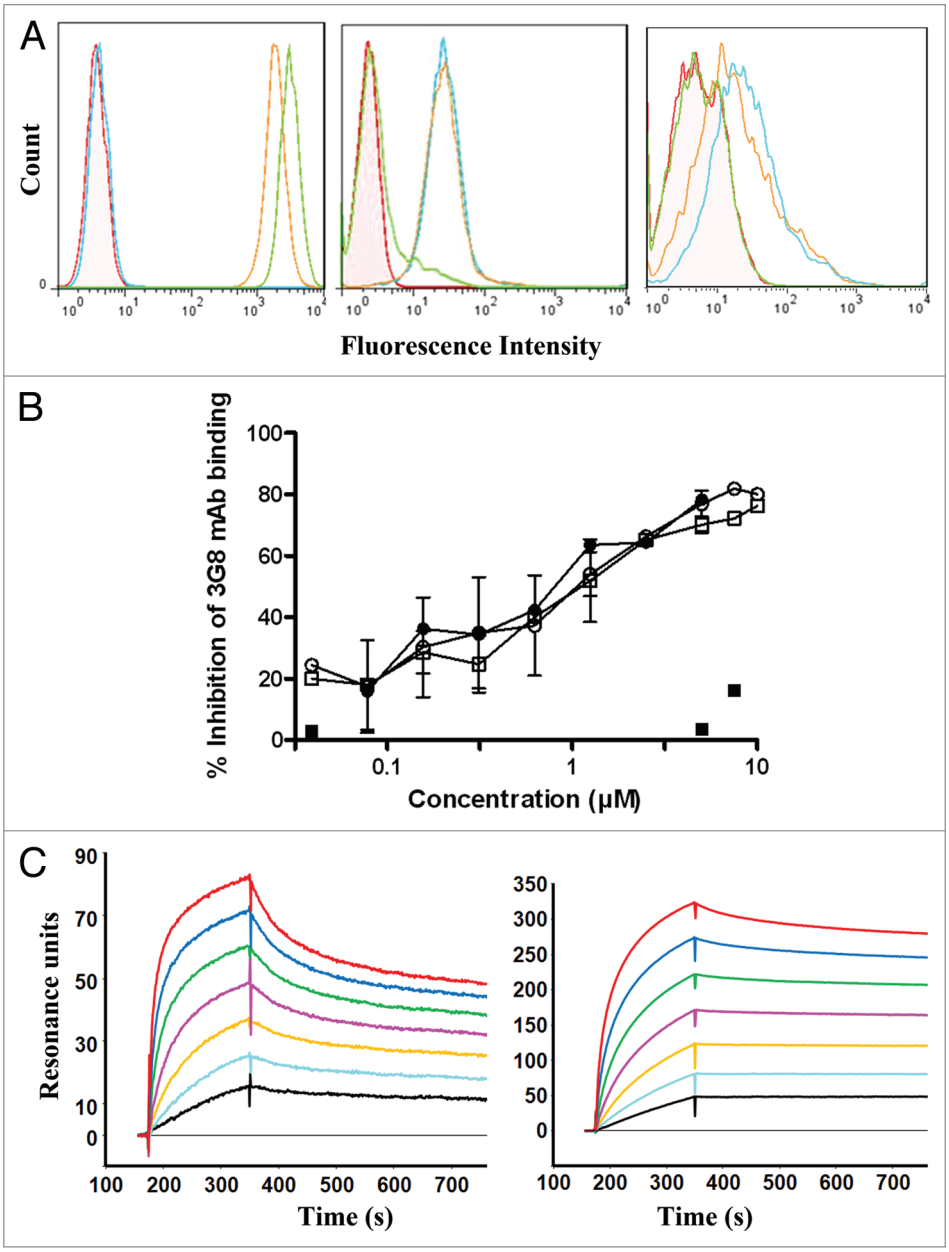

Figure 3. Characterization of the anti-CD20-RLI ICK. **(A)** Specific binding of anti-CD20-RLI and RTX antibodies revealed by flow cytometry: Raji *(left panel)*, Kit225 *(middle panel)* and 32Dβ *(right panel)* cells. Control Ab (filled pink); RTX (green line), anti-CD20-RLI (orange line) and anti-GD2-RLI (blue line). **(B)** Binding of RTX and anti-CD20-RLI to human CD16-transduced NK-92 cells. CD16-transduced NK-92 cells were incubated with varying concentrations of RTX (○), RLI (■), anti-CD20-RLI (□) or the association of RTX and RLI (●) for 30 min at 4 °C followed by FITC-conjugated anti-CD16 3G8 mAb and then analyzed by flow cytometry. Percentages of inhibition of 3G8 binding were calculated as described in "Methods." **(C)** Binding affinities of RLI and anti-CD20-RLI for IL-15Rβ/γ. SPR sensorgrams of binding to immobilized soluble IL-15Rβ/γ with increasing concentrations (3.125, 6.25, 12.5, 25, 50, 100 and 200nM) of RLI (left panel) or anti-CD20-RLI (right panel).

Discussion

This study shows for the first time that targeting CD20 in a disseminated human lymphoma xenograft model with a RLI-based ICK almost completely cures the disease, leading to long-term survival. This anti-tumoral effect is much stronger than those obtained with the naked antibody RTX used at equivalent, and even much higher, doses that only delayed disease onset. Similar antitumor effects have already been reported for an IL-2-based ICK also targeting CD20 on a SCID mouse model,[13] but, as IL-2-based ICKs elicit adverse events similar to those of

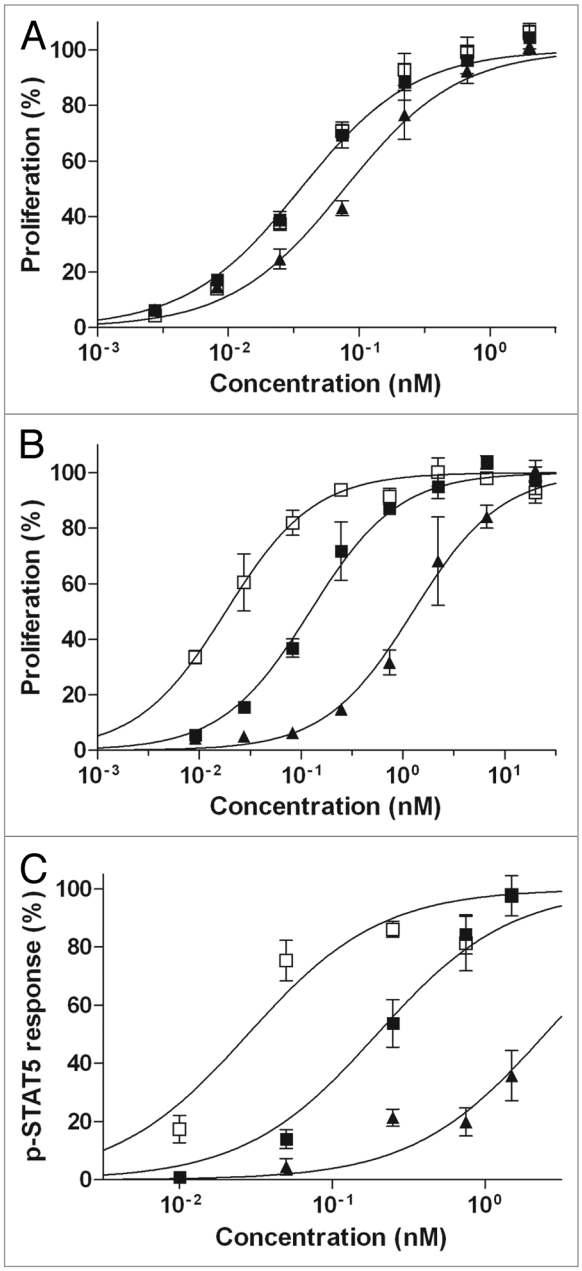

Figure 4. Cytokine-dependent functional effects of anti-CD20-RLI. (**A**) Kit225 or (**B**) 32Dβ cell proliferation induced by increasing concentrations of human IL-15 (▲), RLI (■) or anti-CD20-RLI (□) was assessed by Alamar blue reduction assay. **(C)** Phosphorylation of STAT5 was evaluated in 32Dβ cells stimulated during 30min by increasing concentrations of human IL-15 (▲), RLI (■) or anti-CD20-RLI (□). Data are means ± SEM of three experiments.

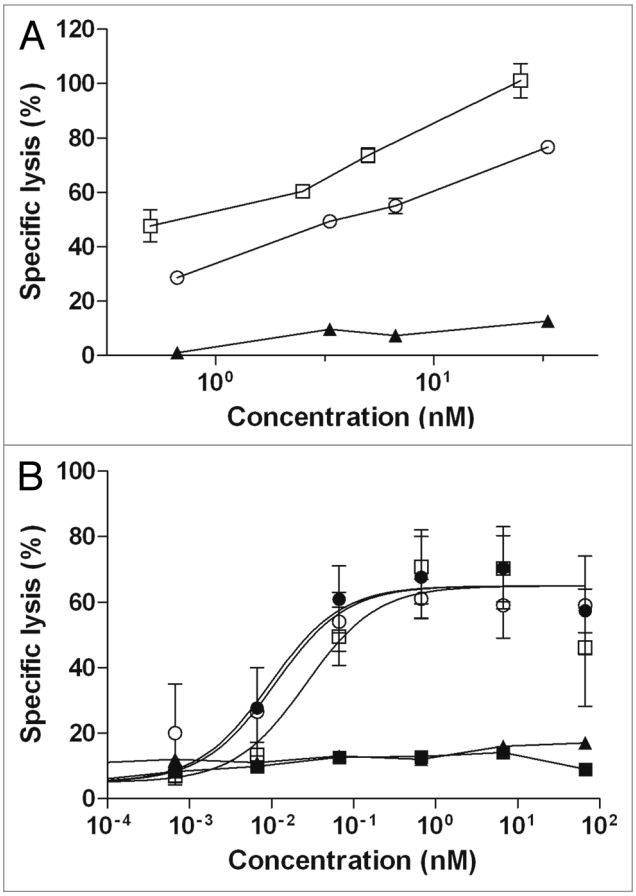

Figure 5. CDC and ADCC activities of anti-CD20-RLI. **(A)** For CDC, CD20 positive Daudi cells were incubated with increasing concentrations of RTX (○), anti-CD20-RLI (□) and anti-GD2 (▲) as a negative control, in the presence of human serum as a source of complement. Lysis of Daudi cells was evaluated using ^{31}Cr release assays. **(B)** ADCC was evaluated on Raji cells at an E/T ratio of 10:1, in the presence of increasing concentrations of RLI (■), RTX (○), RTX + RLI (●), anti-GD2 (▲) and anti-CD20-RLI (□) and using human purified NK cells from healthy donors. Data are means ± SEM of three experiments.

IL-2,[15] anti-CD20-RLI should have the advantage of a better safety profile.[16] Future studies are required to address this point.

We first showed that fusing RLI to the anti-CD20 antibody did not alter the recognition of the CD20 antigen. The cytotoxic effector functions (ADCC, CDC, NK cell activation) of the antibody in vitro or ex-vivo ($CD19^+$ depletion) were also found to be maintained, and even slightly increased in the case of CDC and NK-cell activation. This suggests that fusing RLI to the antibody C-terminus did not decrease the binding of the latter to Fc receptors or complement. The reason for the increased CDC activity and NK cells activation remains to be understood. A direct conformational effect of RLI on C1q recognition appears unlikely as the binding site of C1q on the CH2 domain of the antibody heavy chain is located at a distance of its C-terminus. Concerning NK-cell activation, anti-CD20-RLI and RTX were found to bind similarly to FcγRIIIa expressed by NK cells, indicating that their increased activation is rather the result of a direct effect of RLI than of an increased binding to Fc receptors of the antibody part of the ICK. This is also consistent with the fact that the association of RLI with RTX was as effective as the ICK. This is in agreement with the results from Mogga[27] demonstrating that the direct action of IL-15 on NK cells was responsible for the IL-15-induced increase of RTX-mediated ADCC of PBMCs against CLL cells, and with the recent work of Laprevotte[28] demonstrating that NK cells from CLL patients can be stimulated and expanded by B leukemic cells *trans*-presenting recombinant human IL-15.

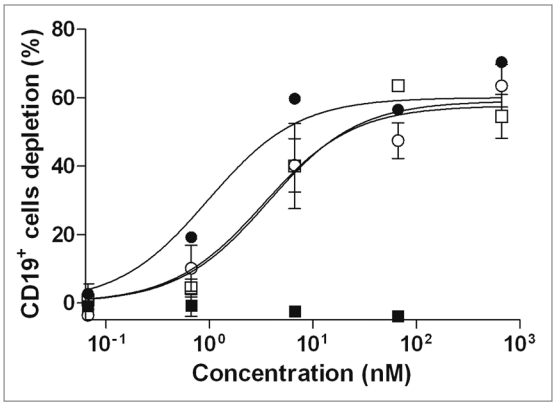

Figure 6. CD19⁺ cells depletion induced by anti-CD20-RLI. Human whole blood from healthy donors was incubated with RLI (■), RTX (○), RTX + RLI (●) and anti-CD20-RLI (□) and CD19⁺ cells depletion was evaluated by flow cytometry. Data are means ± SEM of three experiments.

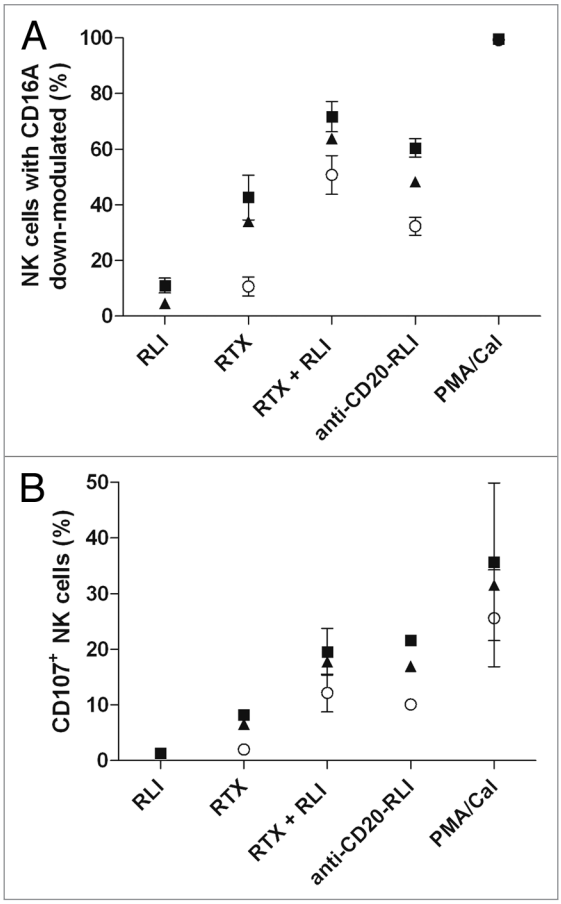

Figure 7. Effect of anti-CD20-RLI on NK-cell activation. CD16A down modulation **(A)** and CD107 expression **(B)** induced by RLI, RTX, RTX + RLI and anti-CD20-RLI (10 μM) were evaluated in human isolated NK cells after 1h (○), 2h (▲) or 3h (■) incubation time. A combination of PMA and Calcium Ionophore was used as positive control. Data are means ± SEM of three experiments.

As previously shown for anti-GD2-RLI,[37] the anti-CD20-RLI ICK kept a binding capacity to cell surface IL-15 receptors, as revealed by flow cytometry. On Kit225 cells, it was found as potent as RLI in inducing cell proliferation. On 32Dβ cells that express the βγ complex, RLI, in agreement with our previous works,[33,37] was about 10-fold more efficient on a molar basis than IL-15 in inducing cell proliferation as well as signal transduction (STAT5 phosphorylation). In this setting that mimics IL-15 *trans*-presentation, anti-CD20-RLI was found even 7-fold more efficient than RLI both to induce STAT5 signaling and cell proliferation. This increased potential is in line with its 3-fold-higher binding affinity for a soluble IL-15Rβ/γ complex compared with RLI, and could reflect the ability of the ICK to engage two RLI binding moieties. As already proposed in the case of the anti-GD2-RLI,[37] this increased efficiency over RLI could reflect a more persistent receptor activation.

The SCID/Raji mouse model, where Raji cells have been inoculated i.v. to SCID mice, has usually been used for the investigation of various therapeutic strategies against NHL. In this model, the association of RLI to RTX in the ICK format was found to spectacularly enhance the RTX anti-tumoral effect. All mice except one receiving the ICK treatment were still alive up to at least 120 d after the inoculation of Raji cells, without any clinical sign of disease, whereas all mice receiving RTX were dead at day 35 with a mean survival of 27 d. Linking RLI to RTX in the ICK format was also essential for this high efficiency, the simple non covalent association of RLI to RTX, although synergistic, only increasing mean survival to 35 d.

Interestingly, the irrelevant ICK (anti-GD2-RLI) was shown to display substantial efficiency, suggesting that a significant part of the ICK antitumor effect is associated with a specific effect of circulating RLI. These results are in agreement with those of Gillies[13] showing that an anti-CD20-IL-2 with decreased ADCC activity (by removal of the N-linked glycan of the antibody) retained significant antitumor activity. Given the fact that RLI treatment alone had no significant effect, they indicate that the enhanced bioavailability of RLI as a result of its fusion to an antibody plays a significant role. Indeed, the serum half-life and AUC of RLI were increased by about 3-fold and 34-fold, respectively, when fused to RTX and similar results were previously found with anti-GD2-RLI.[37] Nonetheless, given the much higher efficiency of anti-CD20-RLI over anti-GD2-RLI in the Raji model, the anti-CD20 component of the ICK has an essential role, targeting the RLI to the tumor site where antibody cytotoxic functions and cytokine-immunostimulatory functions can cooperate. ADCC triggered by human Fc in mouse model has already been evidenced in vivo, using RTX and FCRγ chain-deficient mice[43] or NK cell-depleted mice.[10] The higher in vitro activities of anti-CD20-RLI compared with RLI (7-fold higher proliferative response through IL-15Rβ/γ) or anti-CD20 (higher CDC and NK cells activation) likely participate to this increased in vivo antitumor effect.

As expected, the fusion of RLI to the carboxy-terminus of RTX shortened its circulating half-life (8.5 h vs 100 h), an effect usually observed with immunocytokines[44,45] and depending to some extent on uptake by FCR-bearing cells as well as intracellular proteolysis. In contrast to ch14.18-IL-2 (an anti-GD2-IL-2 fusion protein),[46] proteolytic cleavage of anti-CD20-RLI seems

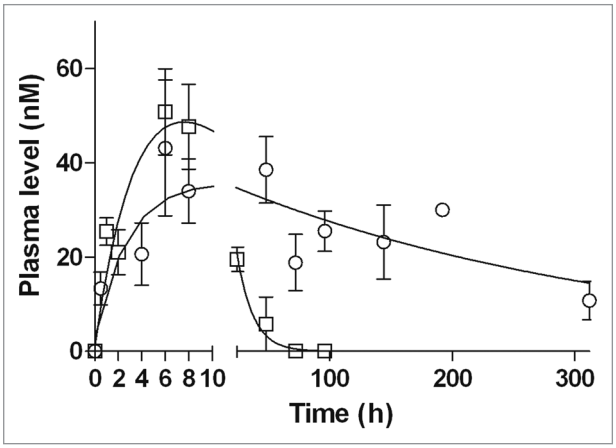

Figure 8. Pharmacokinetic profiles of anti-CD20-RLI. Male C57BL/6 mice were injected with a single i.p. of 16 μg anti-CD20-RLI (□) or 12 μg of RTX (○) and plasma concentrations were determined by ELISA at the indicated points. *, $P < 0.0001$ vs anti-CD20-RLI, F test.

unlikely since similar plasma levels were detected using two ELISA methods that distinguish between the Ab moiety and the intact fusion protein. Given the similar binding of anti-CD20-RLI and RTX to FcγRIIIa, a modification of the recycling through the binding to FcRn could explain the shorter half-life of the ICK, but it remains to be evaluated.

All these results demonstrate the interest of targeting RLI to the tumor site. Furthermore, given the facts that human IgGs will at least bind human FCRγs as efficiently as mouse FcRγs[47] and that human IL-15 is more active on human than mouse NK cells,[48] an even higher effect of the RLI-based ICK may be expected in human. The interest of targeting RLI to the tumor site by the means of an anti-CD20 antibody has not been reported so far. Our study highlights its therapeutic benefits, which are related to the improved pharmacokinetic properties of the cytokine provided by the antibody, together with the preservation and even increased effector properties of the latter (ADCC, CDC, NK cells activation). This synergistic combination should allow a reduction of the therapeutic doses, limit the side effects of both components and improve the clinical efficacy of RTX, particularly in patients with refractory B-cell lymphoma. The better safety profile of IL-15 compared with IL-2 allows considering such fusion proteins as promising drugs in cancer immunotherapy.

RTX resistance in the treatment of B-cell NHL is a common clinical occurrence present in about half of treatment-naïve patients and developing with repeated treatment in the remainder. However, its exact mechanisms remain poorly understood, although potential implication of the three major pathways of RTX action (complement fixation, ADCC, and apoptosis induction) has been proposed.[49] Whereas recognition of antigen-bound RTX by Fc-receptor bearing monocytes appears to lead to CD20-antibody complex shaving (leading to RTX resistance), its recognition by NK cells leads to ADCC (leading to RTX efficacy).[50] Thus, anti-CD20-RLI, by inducing NK cells recruitment and activation at the tumor site through its cytokine moiety, would favor ADCC over shaving. Anti-CD20-RLI would hence be expected to be particularly suitable for patients whose resistance to RTX treatment is known to be related to an ADCC default. However, the SCID CB-17/Raji mouse model used in this report expresses NK cells and myeloid cells but is devoid of the T/B compartments. Further preclinical studies must therefore be performed to take into account the role of the adaptive immune response component and to determine the preclinical toxicity.

Table 1. Summary of the pharmacokinetic parameters of IL-15, RLI, anti-CD20-RLI and RTX in male C57BL/6 mice following a single i.p. administration of a cytokine equivalent molar dose (160pmol)

	RTX	Anti-CD20-RLI	RLI*	IL-15*
Mw (kDa)	150	200	25	13
Dose (μg)	12	16	4	2.4
Dose (pmol)	80	80	160	160
C_{max} (nM)	43.2	50.8	3.4	4.7
T_{max} (h)	6	6	1	0.5
$T_{1/2}$ (h)	100	8.5	3	0.5
AUC (nM.h)	7770	1188	35	5

Mw, molecular weight; Cmax, maximum plasma concentration; Tmax, time to reach maximum plasma concentration; T1/2, half-life; AUC, area under the curve; *Values taken from Bessard et al.[36]

Materials and Methods

Reagents and animals

Seven-week-old male C57BL/6 mice and five-week-old female SCID CB-17 mice were obtained from Janvier and Charles River, respectively. Mice were maintained under pathogen-free conditions and experiments were performed in accordance with French laws and regulations. Recombinant human IL-15 was obtained from Peprotech, Inc. and recombinant human IL-2 from Chiron. Recombinant human IL-15Rβ (224–2B/CF), recombinant human common γ chain (384-RG/CF), murine IL-3, mouse anti-human IL-15 mAb (MAB247) and its biotinylated form (BAM247) were purchased from R&D Systems. RLI was produced as described previously.[33] Control human isotype IgG was purchased from Santa-Cruz Biotechnology, peroxidase-conjugated polyclonal goat anti-human IgG (H+L) (109–036–003) from Jackson ImmunoResearch, anti-human IgG (H+L) (UP892370) from Interchim, mouse anti-human IL-15 mAb (B-E29) from Gen-Probe and RTX, an anti-CD20 mAb from Roche. FITC-conjugated 3G8 mAb specific for CD16, phycoerythrin-conjugated NKH-1 mAbs specific for CD56, phycoerythrin-labeled anti-human anti-CD19 (A07769), FITC-labeled anti-human anti-CD3/phycoerythrin-cyanin5-labeled anti-human anti-CD56 (A07415) were purchased from Beckman Coulter and are mouse IgG1. ScreenSureFire STAT5 (p-Tyr694/699) Assays Kit (TGRS5S500) was from PerkinElmer.

Cell culture

All cell lines were grown at 37 °C under a humidified 5% CO_2 atmosphere. Kit225 T lymphoma human cells,[51] 32Dβ

lymphoblast murine cells,[52] and CD16-transduced NK-92 cells, used to evaluate the binding to CD16, were grown as described previously.[37] The human Raji cell line (ATCC CCL-86) and the human Daudi cell line (ATCC CCL-213) were cultured in RPMI-1640 medium with 10% fetal calf serum (FCS) and 2 mM glutamine. NK cells, used as effector cells in ADCC experiment, were prepared from peripheral blood mononuclear cells of healthy donor of Etablissement Français du Sang of Nantes with the human NK EasySepKit (StemCell Technologies, Inc.). All human cell lines were authenticated less than 6 mo before the end of the experiments by using Promega Power Plex 18 System for DNA testing (DDC).

ICKs plasmids construction

The light chain and the heavy chain sequences of RTX were cloned in pcDNA6 and pcDNA3.1 Hygro, respectively (Life Technologies Ltd). The IL-15 superagonist RLI[33] was fused in frame at the 3′ end of the RTX heavy chain. An irrelevant ICK (anti-GD2-RLI) was also constructed with the heavy and light chains of the anti-GD2 antibody as templates.[37]

ICKs expression and purification

Expression plasmids pcDNA6 blasticidine/anti-CD20-L and pcDNA3.1 HYGRO/anti-CD20-H-RLI were transiently transfected into CHO cells using Polyethyleneimine (Tebu-bio) according to the manufacturer's instructions. ICK production was further conducted in Power CHO-2-CD medium (Lonza). ICK were affinity-purified from culture supernatants by using a HiTrap Protein A HP column (GE Healthcare). The eluted ICK were dialyzed against PBS for buffer exchange, sterile-filtered (0.22 μm), and stored at –80 °C. ICK concentrations were determined by measuring the absorbance at 280nm and their purities were analyzed in NR and R conditions on SDS-PAGE, in R conditions on western blot and in native conditions by Akta purifier 10 gel filtration on a Superdex S-200 size exclusion column (GE Healthcare).

SDS-PAGE and western blot analysis

Purified proteins were analyzed on 4–12% Bis-Tris Gels (Life Technologies), as described previously.[37] For western blot analysis of purified proteins, an anti-human IgG (Interchim UP892370) or an anti-IL-15 mAb (B-E29) were used as primary antibody before a secondary horseradish peroxidase (HRP)-conjugated anti-goat/anti-rabbit or anti-mouse antibody conjugated with HPR.

ELISAs

Anti-CD20-RLI plasma levels were evaluated with two ELISAs. The first ELISA used an anti-human IgG (UP892370) as capture antibody and the biotinylated anti-IL-15 (BAM247) also recognizing the IL-15 moiety in RLI, as revealing antibody. The second used the same capture antibody as above and an anti-IgG antibody (109–036–003) as revealing antibody, and was also used to measure RTX plasma levels. The stability of RLI was demonstrated by silver stain SDS-PAGE under R conditions (**Fig. S1**) and by the fact that RLI maintains its in vitro proliferative activity (**Fig.S2**), after freeze-thaw cycles.

Binding properties of ICKs

For CD20 or IL-15 receptor binding, Raji, Kit225 or 32Dβ (2×10^5) were incubated 1h at 4 °C with either 10 μg/ml anti-CD20-RLI, RTX or control isotype IgG. After reaction with 1.25 μg/ml PE-labeled goat anti-human IgG as a secondary antibody (BD Biosciences), cell fluorescence was measured in a Calibur flow cytometer and data were analyzed using FlowJo Software (BD Biosciences).

The binding to FcγRIIIa expressed at the surface of CD16-transduced NK-92 cells was performed as described previously.[53] In brief, cells (10^5) were incubated with indicated concentrations of RTX, RLI, anti-CD20-RLI or the association of RTX and RLI for 30 min at 4 °C followed by FITC-conjugated anti-CD16 3G8 mAb and analyzed by flow cytometry. Fluorescence analyses were performed using Kaluza 1.2 version (Beckman Coulter). Results were expressed as the percentage of inhibition of 3G8 mAb binding: (MFI in absence of rituximab – MFI in presence of rituximab) × 100 / (MFI in absence of rituximab).[53]

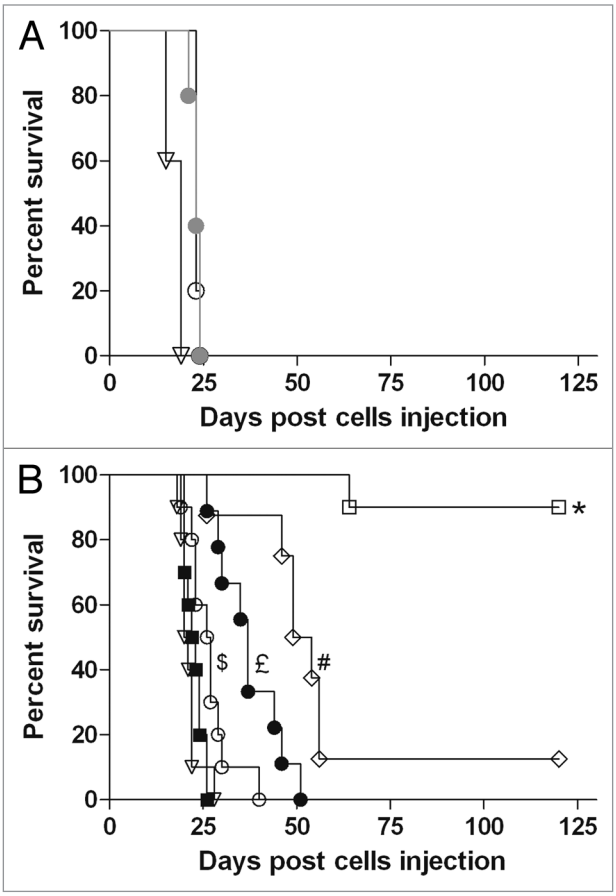

Figure 9. Effect of anti-CD20-RLI on survival of tumor-bearing SCID mice. Mice were inoculated intravenously with Raji cells ($2.5x10^6$). At days 5, 10, 15 and 20 after tumor inoculation, groups of 10 mice were treated with **(A)** saline (open triangle), low dose (12 μg, open circle) or conventional therapeutic dose (200 μg, filled gray circle) of RTX or **(B)** with equimolar dose of saline, RLI (2 μg), RTX (12 μg), RTX + RLI, anti-CD20-RLI (16 μg) or anti-GD2-RLI (16 μg). Mice were monitored daily and sacrificed at the onset of hind leg paralysis. Percent survival of mice after treatment with saline (▽), RLI (■), RTX (○), RTX + RLI (●), anti-CD20-RLI (□) or anti-GD2-RLI (◇). *, $P< 0.001$ vs saline, RLI, RTX, RTX + RLI and anti-GD2-RLI; #, $P< 0.01$ vs, saline, RLI, RTX and RTX + RLI; £, $P< 0.01$ vs saline, RLI and RTX; $, $P< 0.05$ vs saline and RLI, Log-rank test.

The binding to IL-15Rβ/γ was further evaluated by SPR studies. The SPR experiments were performed at 25 °C with a BIAcore 3000 biosensor (GE Healthcare). Recombinant IL-15Rβ and Rγ were covalently linked to CM5 sensor chips using the amine coupling method in accordance with the manufacturer's instructions, and the binding of increasing concentrations of RLI or anti-CD20-RLI was monitored as described.[33] The BIAeval 4.1 software was used to fit data.

Proliferation assays

The proliferative responses of Kit225 and 32Dβ cells to IL-15, RLI or anti-CD20-RLI was assessed by Alamar blue reduction assay (AbDSerotec). Cells were starved in the culture medium without cytokine during 24 h for Kit225 or 4 h for 32Dβ. They were plated at 1×10^4 cells in 100 μl and cultured for 48 h in the medium supplemented with increasing concentrations of IL-15, RLI or anti-CD20-RLI. The effect of RTX (100nM) alone or added to increasing concentrations of anti-CD20-RLI was also evaluated. Alamar blue (10 μl) was added to each well and the fluorescence was measured at excitation 560 nm and emission 590 nm using Fluoroskan Ascent FL reader (Thermo Electro Corporation) after a 6h-incubation period at 37 °C.

Phospho-STAT5 assays

Detection of phospho-STAT5 (p-STAT5) proteins was assessed by AlphaScreenSureFire STAT5 assay kit (PerkinElmer). Exponentially-growing 32Dβ cells were washed and serum-starved to reduce basal phosphorylation (4 h in cytokine-deprived RPMI-1640 medium supplemented with 0.5% FCS and 2 mM glutamine). After 30 min stimulation with increasing concentrations of IL-15, RLI or anti-CD20-RLI at 37 °C, cells were suspended in ice-cold PBS and cell pellets were lysed by the addition of 50 μl of Lysis buffer with shaking for 15 min. A portion of lysate from each condition (4 μl) was transferred to a 384-well ProxiPlate and assayed for p-STAT5. Briefly, a mixture of Reaction buffer, Activation buffer, and AlphaScreen Acceptor beads was prepared under low light conditions according to the manufacturer's instructions, and 5 μl of the assay mixture was added to lysates in each well. The plates were sealed and covered in foil, and incubated at room temperature for 2 h. After this, a mixture of Dilution buffer and AlphaScreen donor beads was prepared under low light conditions, and 2 μl was added to the wells. The plates were sealed and covered in foil, and incubated at room temperature for 2 h. The signal in the wells was then detected using an EnSpire Multimode Plate Reader (Perkin Elmer). Lysates protein concentration was determined by BC Assay Kit (Uptima) using BSA as standard.

ADCC and CDC assays

Lysis of Raji and Daudi cells was evaluated using ^{51}Cr release assays. Target cells (1×10^6) were incubated at 37 °C with 75 μCi ^{51}Cr ($Na_2{}^{51}CrO_4$, Perkin-Elmer) during 1h and washed by centrifugation. CDC and ADCC assays were performed as previously described.[37] NK cells were prepared from donor $CD16^{VV}$ genotype.

B cells depletion assay

Heparinized blood samples (100 μl/well) from healthy human donors were incubated 4h at 37 °C with indicated concentrations of either anti-CD20-RLI, RTX, RLI or the association of RLI and RTX. After a 15min-incubation at room temperature with PE-labeled anti-human anti-CD19, FITC-labeled anti-human anti-CD3 and PE-Cy5-labeled anti-human anti-CD56, cells were analyzed by flow cytometry.

NK-cell activation

For the study of functional responses of NK cells, culture plates were sensitized overnight at 4 °C with a saturating concentration of RTX or anti-CD20-RLI (10 μM) as described.[54] Isolated NK cells (10^5), were laid down in anti-CD20-RLI-sensitized culture plates or in RTX-sensitized culture plates in the absence or in the presence of RLI (10 μM) or in unsensitized culture plates in the presence of a combination of PMA and CaI used as positive control (100 ng/ml and 500 ng/ml respectively). NK cells were incubated for 1, 2 or 3 h at 37 °C with PC5-conjugated anti-CD107a, and then labeled with PC7-conjugated 3G8 (30 min, 4 °C) and analyzed by flow cytometry as described.[54]

Pharmacokinetic experiments

C57BL/6 mice were injected i.p. with molar equivalent dose of anti-CD20-RLI (16 μg) or RTX (12 μg). At various time points (up to 312h), blood samples were taken (3 mice per point) and immediately centrifuged, and the plasma was frozen at –20 °C. Proteins plasma levels were evaluated using two ELISAs (see above) and biodisponibility parameters were calculated using a one-compartment model with GraphPad Prism software.

Tumor model

The procedure (number CEEA-Pdl.2011.36) was approved by French Ethics Committee for animal experimentation number 6. Human lymphoma Raji cells (2.5×10^6) were injected intravenously (i.v.) in SCID mice.[55] Mice (10 mice per group) were then injected i.p. at days 5, 10, 15 and 20 after cells transplantation, with saline or equimolar doses of RLI (2 μg), RTX (12 μg), co-administration of RTX and RLI, anti-CD20-RLI (16 μg) or anti-GD2-RLI (16 μg) as irrelevant ICK. A higher dose of RTX (200 μg) was also tested. Paralysis of mice was considered as the limit point for survival curves.

Statistical analysis

The data are presented as mean ± SEM. The animal survival data were analyzed using Kaplan and Meier survival analysis. Statistical analysis used log-rank test for survival curves and F-test for pharmacokinetic experiments. *P* values of less than 0.05 were considered significant.

Disclosure of Potential Conflicts of Interest

A.Q., D.B., and Y.J. are co-founders and shareholders of Cytune Pharma. The remaining authors declare no competing financial interests.

Acknowledgments

M.V. was supported by fellowships from the Ministère de l'Enseignement Supérieur et de la Recherche and the Association pour la Recherche sur le Cancer. The authors thank Sébastien Morisseau for helpful advices and technical assistance, Karine Bernardeau and Klara Echasserieau (Recombinant Protein Facility) for site-exclusion chromatography analysis, and Virginie Maurier for in vivo technical assistance.

Financial support

INSERM, CNRS, Institut National du Cancer and Cancéropole Grand Ouest (MabImpact), OSEO Innovation and Région Pays de Loire (CIMATH2), Agence Nationale de la Recherche (Investissement d'avenir, LabEx MabImprove ANR-10-LABX53), Ministère de l'Enseignement Supérieur et de la Recherche, Association pour la Recherche sur le Cancer and Ligue contre le Cancer.

Supplemental Materials

Supplemental materials may be found here:
www.landesbioscience.com/journals/mabs/article/28699/

References

1. Molina A. A decade of rituximab: improving survival outcomes in non-Hodgkin's lymphoma. Annu Rev Med 2008; 59:237-50; PMID:18186705; http://dx.doi.org/10.1146/annurev.med.59.060906.220345
2. Hallek M, Fischer K, Fingerle-Rowson G, Fink AM, Busch R, Mayer J, Hensel M, Hopfinger G, Hess G, von Grünhagen U, et al.; International Group of Investigators; German Chronic Lymphocytic Leukaemia Study Group. Addition of rituximab to fludarabine and cyclophosphamide in patients with chronic lymphocytic leukaemia: a randomised, open-label, phase 3 trial. Lancet 2010; 376:1164-74; PMID:20888994; http://dx.doi.org/10.1016/S0140-6736(10)61381-5
3. Ruuls SR, Lammerts van Bueren JJ, van de Winkel JGJ, Parren PWHI. Novel human antibody therapeutics: the age of the Umabs. Biotechnol J 2008; 3:1157-71; PMID:18702090; http://dx.doi.org/10.1002/biot.200800110
4. Cartron G, Watier H, Golay J, Solal-Celigny P. From the bench to the bedside: ways to improve rituximab efficacy. Blood 2004; 104:2635-42; PMID:15226177; http://dx.doi.org/10.1182/blood-2004-03-1110
5. Boross P, Leusen JHW. Mechanisms of action of CD20 antibodies. Am J Cancer Res 2012; 2:676-90; PMID:23226614
6. Davis TA, Grillo-López AJ, White CA, McLaughlin P, Czuczman MS, Link BK, Maloney DG, Weaver RL, Rosenberg J, Levy R. Rituximab anti-CD20 monoclonal antibody therapy in non-Hodgkin's lymphoma: safety and efficacy of re-treatment. J Clin Oncol 2000; 18:3135-43; PMID:10963642
7. Smith MR. Rituximab (monoclonal anti-CD20 antibody): mechanisms of action and resistance. Oncogene 2003; 22:7359-68; PMID:14576843; http://dx.doi.org/10.1038/sj.onc.1206939
8. Shinkawa T, Nakamura K, Yamane N, Shoji-Hosaka E, Kanda Y, Sakurada M, Uchida K, Anazawa H, Satoh M, Yamasaki M, et al. The absence of fucose but not the presence of galactose or bisecting N-acetylglucosamine of human IgG1 complex-type oligosaccharides shows the critical role of enhancing antibody-dependent cellular cytotoxicity. J Biol Chem 2003; 278:3466-73; PMID:12427744; http://dx.doi.org/10.1074/jbc.M210665200
9. Moore GL, Chen H, Karki S, Lazar GA. Engineered Fc variant antibodies with enhanced ability to recruit complement and mediate effector functions. MAbs 2010; 2:181-9; PMID:20150767; http://dx.doi.org/10.4161/mabs.2.2.11158
10. Hernandez-Ilizaliturri FJ, Jupudy V, Ostberg J, Oflazoglu E, Huberman A, Repasky E, Czuczman MS. Neutrophils contribute to the biological antitumor activity of rituximab in a non-Hodgkin's lymphoma severe combined immunodeficiency mouse model. Clin Cancer Res 2003; 9:5866-73; PMID:14676108
11. Gluck WL, Hurst D, Yuen A, Levine AM, Dayton MA, Gockerman JP, Lucas J, Denis-Mize K, Tong B, Navis D, et al. Phase I studies of interleukin (IL)-2 and rituximab in B-cell non-hodgkin's lymphoma: IL-2 mediated natural killer cell expansion correlations with clinical response. Clin Cancer Res 2004; 10:2253-64; PMID:15073100; http://dx.doi.org/10.1158/1078-0432.CCR-1087-3
12. Eisenbeis CF, Grainger A, Fischer B, Baiocchi RA, Carrodeguas L, Roychowdhury S, Chen L, Banks AL, Davis T, Young D, et al. Combination immunotherapy of B-cell non-Hodgkin's lymphoma with rituximab and interleukin-2: a preclinical and phase I study. Clin Cancer Res 2004; 10:6101-10; PMID:15447996; http://dx.doi.org/10.1158/1078-0432.CCR-04-0525
13. Gillies SD, Lan Y, Williams S, Carr F, Forman S, Raubitschek A, Lo K-M. An anti-CD20-IL-2 immunocytokine is highly efficacious in a SCID mouse model of established human B lymphoma. Blood 2005; 105:3972-8; PMID:15692062; http://dx.doi.org/10.1182/blood-2004-09-3533
14. Kontermann RE. Antibody-cytokine fusion proteins. Arch Biochem Biophys 2012; 526:194-205; PMID:22445675; http://dx.doi.org/10.1016/j.abb.2012.03.001
15. Pasche N, Neri D. Immunocytokines: a novel class of potent armed antibodies. Drug Discov Today 2012; 17:583-90; PMID:22289353; http://dx.doi.org/10.1016/j.drudis.2012.01.007
16. Munger W, DeJoy SQ, Jeyaseelan R Sr., Torley LW, Grabstein KH, Eisenmann J, Paxton R, Cox T, Wick MM, Kerwar SS. Studies evaluating the antitumor activity and toxicity of interleukin-15, a new T cell growth factor: comparison with interleukin-2. Cell Immunol 1995; 165:289-93; PMID:7553894; http://dx.doi.org/10.1006/cimm.1995.1216
17. Anderson DM, Kumaki S, Ahdieh M, Bertles J, Tometsko M, Loomis A, Giri J, Copeland NG, Gilbert DJ, Jenkins NA, et al. Functional characterization of the human interleukin-15 receptor alpha chain and close linkage of IL15RA and IL2RA genes. J Biol Chem 1995; 270:29862-9; PMID:8530383; http://dx.doi.org/10.1074/jbc.270.50.29862
18. Giri JG, Kumaki S, Ahdieh M, Friend DJ, Loomis A, Shanebeck K, DuBose R, Cosman D, Park LS, Anderson DM. Identification and cloning of a novel IL-15 binding protein that is structurally related to the alpha chain of the IL-2 receptor. EMBO J 1995; 14:3654-63; PMID:7641685
19. Dubois S, Mariner J, Waldmann TA, Tagaya Y. IL-15Ralpha recycles and presents IL-15 In trans to neighboring cells. Immunity 2002; 17:537-47; PMID:12433361; http://dx.doi.org/10.1016/S1074-7613(02)00429-6
20. Burkett PR, Koka R, Chien M, Chai S, Boone DL, Ma A. Coordinate expression and trans presentation of interleukin (IL)-15Ralpha and IL-15 supports natural killer cell and memory CD8+ T cell homeostasis. J Exp Med 2004; 200:825-34; PMID:15452177; http://dx.doi.org/10.1084/jem.20041389
21. Mortier E, Advincula R, Kim L, Chmura S, Barrera J, Reizis B, Malynn BA, Ma A. Macrophage- and dendritic-cell-derived interleukin-15 receptor alpha supports homeostasis of distinct CD8+ T cell subsets. Immunity 2009; 31:811-22; PMID:19913445; http://dx.doi.org/10.1016/j.immuni.2009.09.017
22. Kennedy MK, Glaccum M, Brown SN, Butz EA, Viney JL, Embers M, Matsuki N, Charrier K, Sedger L, Willis CR, et al. Reversible defects in natural killer and memory CD8 T cell lineages in interleukin 15-deficient mice. J Exp Med 2000; 191:771-80; PMID:10704459; http://dx.doi.org/10.1084/jem.191.5.771
23. Waldmann TA. The biology of interleukin-2 and interleukin-15: implications for cancer therapy and vaccine design. Nat Rev Immunol 2006; 6:595-601; PMID:16868550; http://dx.doi.org/10.1038/nri1901
24. Marks-Konczalik J, Dubois S, Losi JM, Sabzevari H, Yamada N, Feigenbaum L, Waldmann TA, Tagaya Y. IL-2-induced activation-induced cell death is inhibited in IL-15 transgenic mice. Proc Natl Acad Sci U S A 2000; 97:11445-50; PMID:11016962; http://dx.doi.org/10.1073/pnas.200363097
25. Rochman Y, Spolski R, Leonard WJ. New insights into the regulation of T cells by gamma(c) family cytokines. Nat Rev Immunol 2009; 9:480-90; PMID:19543225; http://dx.doi.org/10.1038/nri2580
26. Moga E, Alvarez E, Cantó E, Vidal S, Rodríguez-Sánchez JL, Sierra J, Briones J. NK cells stimulated with IL-15 or CpG ODN enhance rituximab-dependent cellular cytotoxicity against B-cell lymphoma. Exp Hematol 2008; 36:69-77; PMID:17959301; http://dx.doi.org/10.1016/j.exphem.2007.08.012
27. Moga E, Cantó E, Vidal S, Juarez C, Sierra J, Briones J. Interleukin-15 enhances rituximab-dependent cytotoxicity against chronic lymphocytic leukemia cells and overcomes transforming growth factor beta-mediated immunosuppression. Exp Hematol 2011; 39:1064-71; PMID:21864486; http://dx.doi.org/10.1016/j.exphem.2011.08.006
28. Laprevotte E, Voisin G, Ysebaert L, Klein C, Daugrois C, Laurent G, Fournie J-J, Quillet-Mary A. Recombinant human IL-15 trans-presentation by B leukemic cells from chronic lymphocytic leukemia induces autologous NK cell proliferation leading to improved anti-CD20 immunotherapy. J Immunol 2013; 191:3634-40; PMID:23997218; http://dx.doi.org/10.4049/jimmunol.1300187
29. Mortier E, Bernard J, Plet A, Jacques Y. Natural, proteolytic release of a soluble form of human IL-15 receptor alpha-chain that behaves as a specific, high affinity IL-15 antagonist. J Immunol 2004; 173:1681-8; PMID:15265897
30. Dubois S, Patel HJ, Zhang M, Waldmann TA, Müller JR. Preassociation of IL-15 with IL-15R alpha-IgG1-Fc enhances its activity on proliferation of NK and CD8+/CD44high T cells and its antitumor action. J Immunol 2008; 180:2099-106; PMID:18250415
31. Epardaud M, Elpek KG, Rubinstein MP, Yonekura AR, Bellemare-Pelletier A, Bronson R, Hamerman JA, Goldrath AW, Turley SJ. Interleukin-15/interleukin-15R alpha complexes promote destruction of established tumors by reviving tumor-resident CD8+ T cells. Cancer Res 2008; 68:2972-83; PMID:18413767; http://dx.doi.org/10.1158/0008-5472.CAN-08-0045
32. Stoklasek TA, Schluns KS, Lefrançois L. Combined IL-15/IL-15Ralpha immunotherapy maximizes IL-15 activity in vivo. J Immunol 2006; 177:6072-80; PMID:17056533
33. Mortier E, Quéméner A, Vusio P, Lorenzen I, Boublik Y, Grötzinger J, Plet A, Jacques Y. Soluble interleukin-15 receptor alpha (IL-15R alpha)-sushi as a selective and potent agonist of IL-15 action through IL-15R beta/gamma. Hyperagonist IL-15 x IL-15R alpha fusion proteins. J Biol Chem 2006; 281:1612-9; PMID:16284400; http://dx.doi.org/10.1074/jbc.M508624200

34. Bouchaud G, Garrigue-Antar L, Solé V, Quéméner A, Boublik Y, Mortier E, Perdreau H, Jacques Y, Plet A. The exon-3-encoded domain of IL-15ralpha contributes to IL-15 high-affinity binding and is crucial for the IL-15 antagonistic effect of soluble IL-15Ralpha. J Mol Biol 2008; 382:1-12; PMID:18656487; http://dx.doi.org/10.1016/j.jmb.2008.07.019
35. Huntington ND, Legrand N, Alves NL, Jaron B, Weijer K, Plet A, Corcuff E, Mortier E, Jacques Y, Spits H, et al. IL-15 trans-presentation promotes human NK cell development and differentiation in vivo. J Exp Med 2009; 206:25-34; PMID:19103877; http://dx.doi.org/10.1084/jem.20082013
36. Bessard A, Solé V, Bouchaud G, Quéméner A, Jacques Y. High antitumor activity of RLI, an interleukin-15 (IL-15)-IL-15 receptor alpha fusion protein, in metastatic melanoma and colorectal cancer. Mol Cancer Ther 2009; 8:2736-45; PMID:19723883; http://dx.doi.org/10.1158/1535-7163.MCT-09-0275
37. Vincent M, Bessard A, Cochonneau D, Teppaz G, Solé V, Maillasson M, Birklé S, Garrigue-Antar L, Quéméner A, Jacques Y. Tumor targeting of the IL-15 superagonist RLI by an anti-GD2 antibody strongly enhances its antitumor potency. Int J Cancer 2013; 133:757-65; PMID:23354868; http://dx.doi.org/10.1002/ijc.28059
38. Clémenceau B, Vivien R, Pellat C, Foss M, Thibault G, Vié H. The human natural killer cytotoxic cell line NK-92, once armed with a murine CD16 receptor, represents a convenient cellular tool for the screening of mouse mAbs according to their ADCC potential. MAbs 2013; 5:587-94; PMID:23770975; http://dx.doi.org/10.4161/mabs.25077
39. Perdreau H, Mortier E, Bouchaud G, Solé V, Boublik Y, Plet A, Jacques Y. Different dynamics of IL-15R activation following IL-15 cis- or trans-presentation. Eur Cytokine Netw 2010; 21:297-307; PMID:21078585
40. Blasco H, Lalmanach G, Godat E, Maurel MC, Canepa S, Belghazi M, Paintaud G, Degenne D, Chatelut E, Cartron G, et al. Evaluation of a peptide ELISA for the detection of rituximab in serum. J Immunol Methods 2007; 325:127-39; PMID:17651747; http://dx.doi.org/10.1016/j.jim.2007.06.011
41. Plosker GL, Figgitt DP. Rituximab: a review of its use in non-Hodgkin's lymphoma and chronic lymphocytic leukaemia. Drugs 2003; 63:803-43; PMID:12662126; http://dx.doi.org/10.2165/00003495-200363080-00005
42. McLaughlin P, Grillo-López AJ, Link BK, Levy R, Czuczman MS, Williams ME, Heyman MR, Bence-Bruckler I, White CA, Cabanillas F, et al. Rituximab chimeric anti-CD20 monoclonal antibody therapy for relapsed indolent lymphoma: half of patients respond to a four-dose treatment program. J Clin Oncol 1998; 16:2825-33; PMID:9704735
43. Clynes RA, Towers TL, Presta LG, Ravetch JV. Inhibitory Fc receptors modulate in vivo cytotoxicity against tumor targets. Nat Med 2000; 6:443-6; PMID:10742152; http://dx.doi.org/10.1038/74704
44. Gillies SD, Lan Y, Lo KM, Super M, Wesolowski J. Improving the efficacy of antibody-interleukin 2 fusion proteins by reducing their interaction with Fc receptors. Cancer Res 1999; 59:2159-66; PMID:10232603
45. Gillies SD, Lo K-M, Burger C, Lan Y, Dahl T, Wong W-K. Improved circulating half-life and efficacy of an antibody-interleukin 2 immunocytokine based on reduced intracellular proteolysis. Clin Cancer Res 2002; 8:210-6; PMID:11801561
46. Kendra K, Gan J, Ricci M, Surfus J, Shaker A, Super M, Frost JD, Rakhmilevich A, Hank JA, Gillies SD, et al. Pharmacokinetics and stability of the ch14.18-interleukin-2 fusion protein in mice. Cancer Immunol Immunother 1999; 48:219-29; PMID:10478638; http://dx.doi.org/10.1007/s002620050569
47. Bruhns P. Properties of mouse and human IgG receptors and their contribution to disease models. Blood 2012; 119:5640-9; PMID:22535666; http://dx.doi.org/10.1182/blood-2012-01-380121
48. Eisenman J, Ahdieh M, Beers C, Brasel K, Kennedy MK, Le T, Bonnert TP, Paxton RJ, Park LS. Interleukin-15 interactions with interleukin-15 receptor complexes: characterization and species specificity. Cytokine 2002; 20:121-9; PMID:12453470; http://dx.doi.org/10.1006/cyto.2002.1989
49. Rezvani AR, Maloney DG. Rituximab resistance. Best Pract Res Clin Haematol 2011; 24:203-16; PMID:21658619; http://dx.doi.org/10.1016/j.beha.2011.02.009
50. Beum PV, Kennedy AD, Williams ME, Lindorfer MA, Taylor RP. The shaving reaction: rituximab/CD20 complexes are removed from mantle cell lymphoma and chronic lymphocytic leukemia cells by THP-1 monocytes. J Immunol 2006; 176:2600-9; PMID:16456022
51. Hori T, Uchiyama T, Tsudo M, Umadome H, Ohno H, Fukuhara S, Kita K, Uchino H. Establishment of an interleukin 2-dependent human T cell line from a patient with T cell chronic lymphocytic leukemia who is not infected with human T cell leukemia/lymphoma virus. Blood 1987; 70:1069-72; PMID:3115332
52. Nakamura Y, Russell SM, Mess SA, Friedmann M, Erdos M, Francois C, Jacques Y, Adelstein S, Leonard WJ. Heterodimerization of the IL-2 receptor beta- and gamma-chain cytoplasmic domains is required for signalling. Nature 1994; 369:330-3; PMID:8183373; http://dx.doi.org/10.1038/369330a0
53. Dall'Ozzo S, Tartas S, Paintaud G, Cartron G, Colombat P, Bardos P, Watier H, Thibault G. Rituximab-dependent cytotoxicity by natural killer cells: influence of FCGR3A polymorphism on the concentration-effect relationship. Cancer Res 2004; 64:4664-9; PMID:15231679; http://dx.doi.org/10.1158/0008-5472.CAN-03-2862
54. Congy-Jolivet N, Bolzec A, Ternant D, Ohresser M, Watier H, Thibault G. Fc gamma RIIIa expression is not increased on natural killer cells expressing the Fc gamma RIIIa-158V allotype. Cancer Res 2008; 68:976-80; PMID:18281470; http://dx.doi.org/10.1158/0008-5472.CAN-07-6523
55. Wu L, Wang C, Zhang D, Zhang X, Qian W, Zhao L, Wang H, Li B, Guo Y. Characterization of a humanized anti-CD20 antibody with potent antitumor activity against B-cell lymphoma. Cancer Lett 2010; 292:208-14; PMID:20056316; http://dx.doi.org/10.1016/j.canlet.2009.12.004